Adv. Polar Upper Atmos. Res., **17**, 146–154, 2003

Research note

Second harmonics of auroral kilometric radiation observed by the Akebono satellite

Akira Hosotani, Takayuki Ono, Masahide Iizima and Atsushi Kumamoto

Department of Geophysics, Graduate School of Science, Tohoku University, Aoba, Aramaki, Aoba-ku, Sendai 980-8578

(Received January 8, 2003; Accepted June 5, 2003)

Abstract: The second harmonic wave properties of auroral kilometric radiation (AKR) were examined using data obtained by the Akebono satellite. The results of our statistical analysis indicate that the probability of a harmonic event occurrence is more than 60% of all AKR events. The relationship between the frequencies of the fundamentals and the second harmonics is exactly two times for the upper and lower cut-off frequencies of the spectra as well as the fine structures, within the resolution of the Akebono observations. The intensity ratio of the second harmonics to the fundamentals exhibits a two-fold nature, with both a linear and a quadratic relationship. Further data analyses also revealed that the second harmonic waves of AKR, which propagate in the X-mode, are generated from a source that is identical to that of the fundamental waves that propagate in the O-mode. These results suggest that the mechanism of AKR harmonic structure generation should allow the coexistence of different AKR emission processes.

key words: auroral kilometric radiation, harmonics, Akebono

1. Introduction

Auroral kilometric radiation (AKR) is the most prominent natural radio emission emitted from high-altitude regions of the Earth's polar ionosphere aligned along a field line of an auroral discrete arc (Gurnett, 1974). AKR is dominated by intense X-mode waves, but multiple propagation modes have also been confirmed. For example, Oya and Morioka (1983) identified O-mode waves using Jikiken satellite observations. The coexistence of both X-mode and O-mode waves was also shown by DE 1 satellite observations (Shawhan and Gurnett, 1982). AKR has also been characterized by its spectral features. The harmonic structure of AKR spectra has been reported by Benson (1982, 1985), Mellott *et al.* (1986), and Oya (1990).

The harmonic structure of AKR was first reported by Benson and Calvert (1979), based on the analysis of ISIS 1 ionograms. They initially concluded that the harmonic structure was caused by a nonlinear response of the receiver because the intensity of the AKR occasionally exceeded the saturation level of the receiver. However, Benson (1982) subsequently identified the existence of harmonic structures for weaker AKR

signals, whose intensity was well below the saturation level of the receiver. In other words, the harmonic structure of AKR was recognized to be a natural phenomenon. The detailed properties of the harmonic structure were clarified by an analysis of DE 1 polarization measurements performed by Mellott *et al.* (1986). The results of the analysis were as follows: (1) the second harmonic waves and the fundamental waves propagated in different modes, that is, the fundamental waves propagated in O-mode, and the second harmonic waves propagated in X-mode; (2) harmonic structured AKR events were quite rare; (3) the ratio between the frequencies of the second harmonics and the fundamentals was 1.9 ± 0.2; (4) the ratio between the intensities of the second harmonics and the fundamentals was on the order of 0.1 to 10; and (5) the fundamental waves and the second harmonic waves arrived from similar positions.

Several generation mechanisms can theoretically explain the difference between the propagation modes of the fundamentals and the second harmonics. These mechanisms can be classified into two categories: one, interactions caused by cyclotron resonance, and two, nonlinear wave-wave interactions. The most likely mechanism for the generation of the second harmonic waves is cyclotron maser instability (CMI) (Lee *et al.*, 1980; Wu and Qiu, 1983; Melrose *et al.*, 1984); this mechanism was initially proposed by Wu and Lee (1979) and is believed to generate intense X-mode AKR. The CMI mechanism was applied to explain the harmonic structure of background plasma regions observed by the DE 1 satellite. These regions were denser than the source regions that emit intense X-mode AKR waves. Alternatively, the difference in the propagation modes of the fundamentals and second harmonics of AKR could also be explained by nonlinear wave-wave interactions among upper hybrid waves. This generation mechanism has been used to explain the harmonic structure of terrestrial hectometeric radiation (THR), as proposed by Iizima and Oya (2002). This mechanism could also be applied to the generation of X-mode waves at twice the frequency of the upper hybrid frequency under a head-on collision condition for the upper hybrid waves. In this case, the linear mode conversion mechanism of the upper hybrid waves would produce the fundamental waves that propagate in O-mode.

An AKR spectrum with a harmonic structure was observed by the Akebono satellite, as reported by Oya (1990). The spectrum showed the same relationship between the propagation modes of the fundamentals and the harmonics as was observed by the DE 1 satellite. Since the Akebono satellite observations have higher frequency and time resolutions than those of the DE 1 satellite, the Akebono data enabled the harmonic structures of AKR to be examined in greater detail. The present paper describes several newly observed properties of the harmonic structure of AKR based on a data analysis of the plasma wave observations obtained by the Akebono satellite.

2. Instrumentation and observations

The Akebono satellite was launched into an eccentric polar orbit with an initial apogee and perigee of 10471 km and 272 km, respectively, an inclination of 75.1°, and an orbital period of 212 min. The plasma wave and sounder (PWS) instrumentation onboard the Akebono satellite is able to provide the spectra of right-handed (I_R) and left-handed (I_L) polarization waves with respect to the spin axis of the satellite, which is

towards the sun, within a frequency range of 20 kHz to 5.2 MHz. The polarization spectra data obtained using this equipment was then analyzed to identify the propagation mode of the electromagnetic waves.

Figure 1 shows the typical dynamic spectrum of an AKR event with a harmonic structure observed within the time period from 1640 to 1740 UT on March 13, 1990. The figure utilize a color code to show the intensity of the major axis (top) and the axial ratio $(I_R - I_L)/(I_R + I_L)$ (bottom) of the polarization parameters. The solid curves plotted in the spectra give the electron cyclotron frequency at the satellite position. The axial ratio was applied to identify the propagation mode of the electromagnetic waves based on several assumptions. The source region of the AKR events in Fig. 1 seemed to exist in the vicinity of the satellite position at 1710 UT. The propagation modes of two emissions within frequency ranges of 100 to 200 kHz and 200 to 400 kHz at 1725 UT were identified as O-mode and X-mode, respectively, because they arrived from the positive direction of the z axis of the satellite coordinates, which was identical to the direction of the background magnetic field at this time. In Fig. 1, three propagation characteristics of the AKR event can be pointed out: (1) intense X-mode waves exceeded the saturation level of the receiver in the frequency range of 100 to 270 kHz within the period of 1703 to 1719 UT; (2) O-mode waves with an intensity at least 10 dB weaker than the saturation level were seen in a similar frequency range during

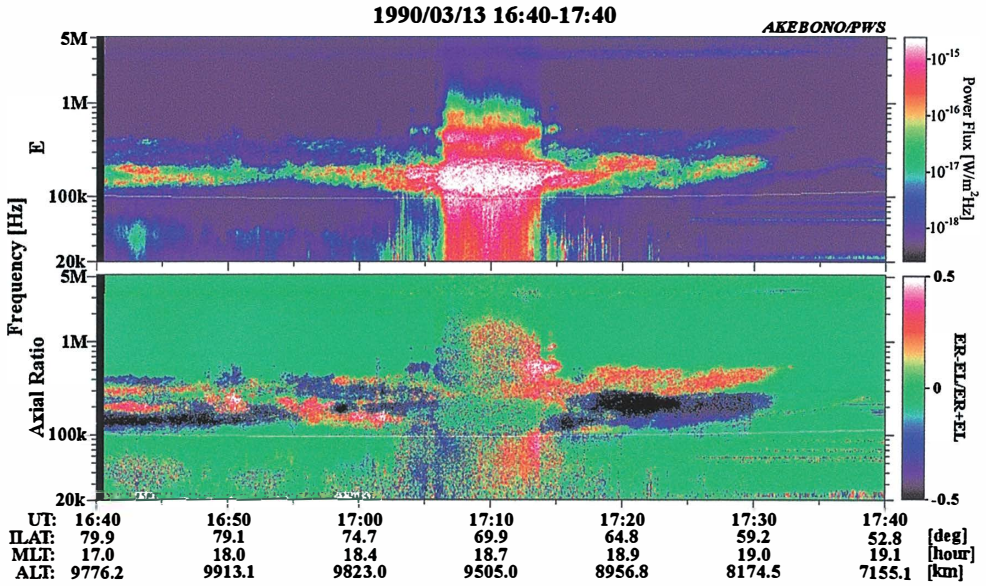

Fig. 1. Dynamic spectrum of a typical AKR event with a harmonic structure that occurred between 1640 and 1740 UT on March 13, 1990. The intensity of the major axis (top) and the axial ratio (bottom) of the polarization parameters are displayed using the colors shown on the right side of the figure. The vertical axis represents the observed frequencies from 20 kHz to 5.2 MHz, with a logarithmic scale. The solid curves show the electron cyclotron frequency at the satellite's position. AKR harmonic structures were seen during the periods of 1640 to 1703 UT and 1719 to 1735 UT.

time periods other than those in which the intense X-mode waves occurred; and (3) the second harmonic waves propagating in the X-mode were about 20 dB weaker than the O-mode waves in the fundamental frequency. The opposite polarization characteristics of the propagation modes in the present harmonic structure were clearly indicated by the difference in the axial ratio. Within the period of 1640 to 1700 UT, the axial ratio changed to the opposite sign; this was caused by the relationship between the positions of the satellite and the source region. The second harmonic waves also changed to a polarization mode that was opposite to that of the fundamental waves. Importantly, the intensity of the fundamental waves was weaker than the saturation level (2.7×10^{-15} ($W/m^2\cdot Hz$)) of the receiver. Therefore, we concluded that the harmonic event observed by the Akebono satellite was a natural phenomenon.

2.1. Occurrence probability of AKR second harmonics

The occurrence probability of second harmonic AKR was examined by analyzing polarization spectra data obtained by the Akebono satellite from 1989 to 1994. We identified harmonic events using the following criteria: (1) the fundamental and second harmonic waves were simultaneously observed, (2) the structures of the two emissions were similar, and (3) a plasma wave with an intensity exceeding the satulation level of the receiver was not simultaneously observed. Using this analysis method, all of the events were found to exhibit fundamentals and second harmonics propagating in the O-mode and X-mode, respectively. Table 1 shows the number of AKR events, the number of events with a harmonic structure, and the occurrence probability of a harmonic event amongst all AKR events. As shown in Table 1, the occurrence probability of second harmonic AKR was more than 60%. Since harmonic waves have relatively weak intensities, as shown in Fig. 1, some harmonic waves may exist below the threshold level of the receiver. Thus, the apparently high probability of harmonic AKR suggests that second harmonic AKR is a basic characteristic of the AKR phenomena. This result seems to contradict the results of the analysis of DE 1 observations that was performed by Mellott *et al.* (1986). This contradiction can be attributed to the difference in the frequency ranges covered by the DE 1 and Akebono satellites, which cover frequency ranges of 2 Hz to 400 kHz and 20 kHz to 5.2 MHz, respectively. In the present analysis, most of the harmonic waves were identified at frequencies over 400 kHz. Thus, the DE 1 receiver was not able to detect the majority

Table 1. The number of AKR events, the number of events with a harmonic structure, and the occurrence probability of a harmonic event for observation data obtained between 1989 and 1994.

Year	AKR events	Harmonic events	Occurrence probability (%)
1989	692	454	65.6
1990	526	269	51.1
1991	584	350	59.9
1992	479	341	71.2
1993	460	246	53.3
1994	508	374	73.6
1989–1994	3249	2034	62.6

of second harmonic AKR waves and only observed those events occurring in a lower frequency range of the AKR spectra.

2.2. Relationship between fundamentals and second harmonics of AKR

To examine the spectral frequency and intensity characteristics of AKR waves, the relationship between the fundamental and second harmonic waves was analyzed for AKR occurring in the period of 0525 to 0555 UT on April 22, 1989 (Fig. 2). Figure 3 compares the spectra of the fundamental (the solid line) and second harmonic (the dashed line) bands at 0532:30 UT by adjusting the horizontal axes to show the harmonic relation between the frequencies of the two emissions. The spectral structure shows a strong harmonic relationship for each fine structure as well as the frequency ranges of the banded emissions involved in the fine structures. Some of the fine structures of the fundamental bands cannot be seen in the second harmonics, however, because of differences in the steps at which observations were made in the frequency ranges of each emission; the frequency range of the second harmonic was observed using a frequency step that was about three times wider than the frequency step used for the fundamental wave observations; this relation is shown in Table 2. After a detailed analysis, we concluded that the second harmonic waves appeared at a frequency that was exactly two times that of the fundamental waves, within the limits of the frequency resolution of the Akebono satellite.

Figure 4 shows the relationship between the intensities of the fundamentals and the

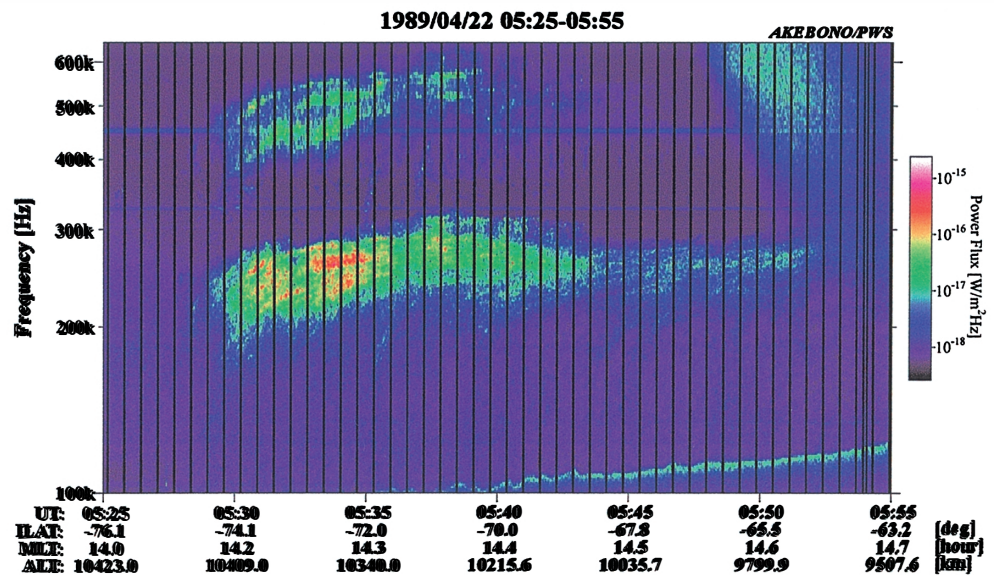

Fig. 2. Dynamic spectrum observed during the period of 0525 to 0555 UT on April 22, 1989. The figure's format is the same as that show in the upper panel of Fig. 1 except for the frequency range. The absent periods of spectra are periods during which other observation modes of the PWS were in operation. Fundamentals and second harmonics were seen within the frequency ranges of 180 to 310 kHz and 360 to 600 kHz, respectively.

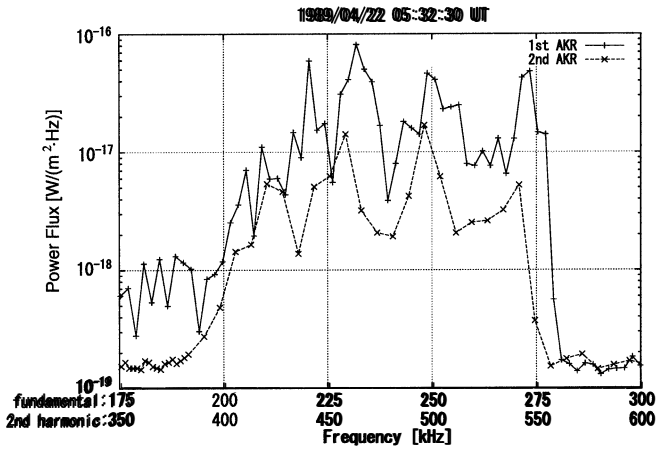

Fig. 3. Spectra of the fundamentals and second harmonics observed at 0532:30 UT. The horizontal axes of the fundamental waves (solid line) and the second harmonic waves (dashed line) have been adjusted to reveal the harmonic relationship.

Table 2. Relationship between the AKR spectra shown in Fig. 3 and the frequency resolution of the PWS receiver.

Frequency range	20 kHz ≀ 140 kHz	141 kHz ≀ 383 kHz	383 kHz ≀ 1.34 MHz	1.34 MHz ≀ 5.20 MHz
Reciever bandwidth	1.0 kHz	1.0 kHz	1.0 kHz	1.0 kHz
Frequency step	945 Hz	1.89 kHz	7.56 kHz	30.2 kHz
AKR spectra	second harmonics in Fig. 3 ◀——▶		fundamentals in Fig. 3 ◀——▶	

second harmonics for the set of fine structures that had the highest frequency in Fig. 3. The fundamental structure drifts in the frequency range of 249 kHz to 279 kHz, and the second harmonic structure drifts in the frequency range of 296 kHz to 556 kHz. The intensity ratios between the fundamentals and the second harmonics produce widely scattered values, as shown in Fig. 4, because the observation frequencies of the PWS receiver were not always sufficient to determine the exact harmonic relation between the fundamentals and the second harmonics. However, the intensity of the second harmonics obviously seems to be correlated with the fundamentals. To clarify this relationship, we plotted two reference lines that may provide useful information concerning the generation mechanisms. The first reference line is the solid line that represents a linear relation between the intensity of the fundamentals and the second harmonics. The second reference line is the dashed line, representing a nonlinear relation between the second harmonics and the square of the fundamentals' intensity. Comparing the two reference lines, most of the data points tend to satisfy a linear relationship. However, for some of the intense AKR waves, a significant number of data points tend to satisfy a quadratic line.

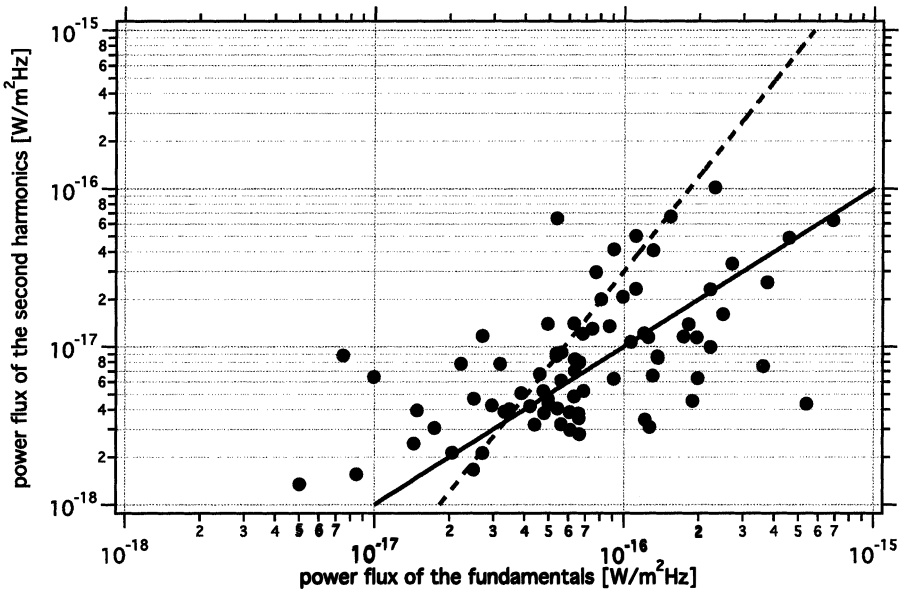

Fig. 4. Scatter plot of the fundamental versus second harmonic intensities of the corresponding fine structures of the AKR spectra shown in Fig. 2. The two reference lines indicate a linear (solid line) and a nonlinear (dashed line) relationship between the intensities of the fundamentals and the second harmonics.

3. Discussion and summary

The properties of second harmonic AKR obtained in the present data analyses can be summarized as follows:

(1) The probability of an AKR event with second harmonic waves was more than 60% of all AKR events. This high probability of occurrence suggests that second harmonic waves are generated as a basic property of AKR generation processes.

(2) The frequency of the second harmonics was exactly twice that of the fundamentals, within the resolution of the Akebono satellite receiver.

(3) The intensities of the second harmonics exhibited either a linear or a quadratic relationship to that of the fundamentals. A quadratic relationship was more often seen for intense AKR waves.

Results (1) and (2) provide information on the physical processes responsible for the generation of harmonic waves in the source region of the AKR. Because AKR waves were emitted from a low-density region of the plasma medium at a frequency closely related to the local electron cyclotron frequency, both the fundamental waves propagating in O-mode and the second harmonic waves propagating in X-mode have a refractive index of about one unit in the source region. Thus, the second harmonic waves propagating in X-mode should travel along almost the same ray path as the fundamental O-mode AKR waves. Consequently, the identical harmonic relationship of the fine structure spectra suggests that both the fundamental and second harmonics

are emitted from the same region. Additionally, the high probability of harmonic AKR suggests that in any AKR emission, O-mode waves are generated at the frequency of the fundamental band, although intense X-mode radio emissions from the central region of the AKR source may occur simultaneously. We concluded that the source region of the AKR contains two types of generation mechanisms: one for the generation of intense X-mode waves and the other for the generation of the O-mode waves and the second harmonic waves that propagate in X-mode. However, the detailed spatial distribution of the intense X-mode source and the O-mode source was not clearly resolved in the present study and remains a topic for future studies.

Result (3) suggests an important characteristic of the generation mechanism responsible for harmonic AKR. At high AKR intensities, the presence of two kinds of intensity relationships, a linear relationship and a quadratic relationship, becomes clear. We considered two generation mechanisms for harmonic AKR that have been previously predicted to generate second harmonic waves: CMI and nonlinear wave-wave interactions of upper hybrid waves. Harmonic AKR with both a linear and a quadratic intensity relationship cannot be explained by either of these generation mechanisms because CMI and nonlinear wave-wave interactions are characterized by either a linear or a nonlinear for relationship between the intensities of the fundamentals and second harmonics, but not both. Therefore, linear and nonlinear generation mechanisms may coexist in the source region. Thus, the coexistence of different processes should be considered in future models of AKR emission.

Acknowledgments

We would like to thank all the members of the Akebono satellite team.

The editor thanks Dr. N. Sato and another referee for their help in evaluating this paper.

References

Benson, R.F. (1982): Harmonic auroral kilometric radiation of natural origin. Geophys. Res. Lett., **9**, 1120–1123.

Benson, R.F. (1985): Auroral kilometric radiation: Wave modes, harmonics, and source region electron density structures. J. Geophys. Res., **90**, 2753–2784.

Benson, R.F. and Calvert, W. (1979): ISIS 1 observations at the source of auroral kilometric radiation. Geophys. Res. Lett., **6**, 479–482.

Gurnett, D.A. (1974): The earth as a radio source: Terrestrial kilometric radiation. J. Geophys. Res., **79**, 4227–4238.

Iizima, M. and Oya, H. (2002): The origin of harmonic generation of terrestrial hectometric radiation. submitted to Earth Planet. Sci.

Lee, L.C., Kan, J.R. and Wu, C.S. (1980): Generation of auroral kilometric radiation and the structure of the auroral acceleration region. Planet. Space Sci., **28**, 703–711.

Mellott, M.M., Huff, R.L. and Gurnett, D.A. (1986): DE 1 observations of harmonic auroral kilometric radiation. J. Geophys. Res., **91**, 13732–13738.

Melrose, D.B., Hewitt, R.G. and Dulk, G.A. (1984): Electron cyclotron maser emission: Relative growth and damping rates for different modes and harmonics. J. Geophys. Res., **89**, 897–904.

Oya, H. (1990): Origin of auroral kilometric radiation as conversion of the upper hybrid mode plasma waves.

Proc. Jpn. Acad., **66**, 129–134.
Oya, H. and Morioka, A. (1983): Observational evidence of Z and L-O mode waves as the origin of auroral kilometric radiation from the Jikiken (EXOS-B) satellite. J. Geophys. Res., **88**, 6189–6203.
Shawhan, S.D. and Gurnett, D.A. (1982): Polarization measurements of auroral kilometric radiation by Dynamics Explorer-1. Geophys. Res. Lett., **9**, 913–916.
Wu, C.S. and Lee, L.C. (1979): A theory of the terrestrial kilometric radiation. Astrophys. J., **230**, 621–626.
Wu, C.S. and Qiu X.M. (1983): Emissions of second-harmonic auroral kilometric radiation. J. Geophys. Res., **88**, 10072–10080.